



Solving the Standard Micromagnetic Problems using Unstructured Meshes with MagTense

Poulsen, E.B.; Insinga, A.R.; Bjørk, R.

Publication date:
2022

Document Version
Publisher's PDF, also known as Version of record

[Link back to DTU Orbit](#)

Citation (APA):
Poulsen, E. B., Insinga, A. R., & Bjørk, R. (2022). *Solving the Standard Micromagnetic Problems using Unstructured Meshes with MagTense*. 468-468. Abstract from 15th Joint MMM-Intermag Conference, New Orleans, United States.

General rights

Copyright and moral rights for the publications made accessible in the public portal are retained by the authors and/or other copyright owners and it is a condition of accessing publications that users recognise and abide by the legal requirements associated with these rights.

- Users may download and print one copy of any publication from the public portal for the purpose of private study or research.
- You may not further distribute the material or use it for any profit-making activity or commercial gain
- You may freely distribute the URL identifying the publication in the public portal

If you believe that this document breaches copyright please contact us providing details, and we will remove access to the work immediately and investigate your claim.

HOM-10. Solving the Standard Micromagnetic Problems using Unstructured Meshes with MagTense. E.B. Poulsen¹, A.R. Insinga¹ and R. Bjørk¹. *1. Technological University of Denmark, Copenhagen, Denmark*

Micromagnetics requires calculation of the demagnetization field, anisotropy field, applied field and exchange field. With the MagTense framework, demagnetization is calculated analytically [1] and both anisotropy and applied field are local, leaving only the exchange field in the form of a second order partial derivative. Standard micromagnetics are limited to finite element methods with large, extraneous simulation volumes or finite difference methods with homogeneous simulation grids, as the demagnetization is calculated using a fast Fourier transform [2], but with MagTense, no such limitation exists. However, here an optimal method of calculating second order partial derivatives on arbitrary meshes in micromagnetics must be determined, continuing previous research [3]. We present solutions to the mumag standard micromagnetic problems (mumag) 3[4] and 4[5] using a direct second order partial derivative technique on four different meshes: Prismatic, tetrahedral, grained prismatic and grained tetrahedral. The grained meshes consist of voronoi generated and Lloyd iterated grain regions with lower resolution towards the center and higher towards the edges, along with high resolution intergrain regions. In fig. 1a) is shown an example of a grained prismatic mesh with 9 grains and an intergrain region in gray. Of course, in the mumag standard problems considered, all regions have the same material properties, but it is easy to envision scenarios where they do not. In fig. 1b) is shown the exchange crossover length of mumag 3 as a function of resolution for three different meshes compared to published solutions. All mesh types converge to the correct value, with the tetrahedral meshes converging faster. In fig. 2 is shown the error compared to published solutions of mumag 4 as a function of resolution using regular-, 4 grained- and 9 grained prismatic meshes. The unstructured meshes converge to the correct result in a way similar to a regular grid. In both cases it is apparent that while for these problems grained meshes offer few advantages, they are nonetheless correctly implemented and open up a slew of possibilities for accurately simulating complex geometries with far fewer elements in irregular meshes.

[1] R. Bjørk and K. K. Nielsen. Magtense - a micromagnetism and magnetostatic framework. doi.org/10.11581/DTU:00000071, <https://www.magtense.org>, 2019 [2] A. Vansteenkiste, Ben Van de Wiele, Journal of Magnetism and Magnetic Materials, 323(21):2585–2591, 2011 [3] Emil Poulsen (Nov 03 2020). P3-03 Micromagnetic Exchange Field Calculations for Unstructured Meshes, The 65th Annual Conference on Magnetism and Magnetic Materials, Underline Science Inc. Accessed July 1st, 2021. <https://underline.io/3924-p3-03---micromagnetic-exchange-field-calculations-for-unstructured-meshes> [4] μ MAG Standard Problem 3 Solutions, Accessed on July 1st, 2021. <https://www.ctcms.nist.gov/~rdm/results3.html> [5] μ MAG Standard Problem 4 Solutions, Accessed on July 1st, 2021. <https://www.ctcms.nist.gov/~rdm/std4/results.html>

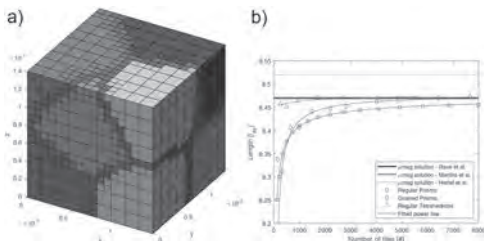


Fig. 1

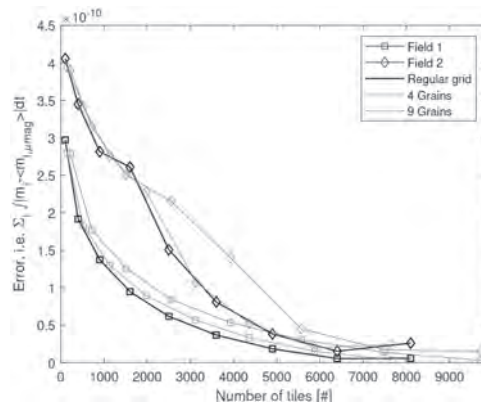


Fig. 2

HOM-11. Effects of α_1 -phase Branch Shapes on Coercivity of Rare-earth Free Alnico Permanent Magnet. H. Won¹, Y. Hong¹, M. Choi¹, G. Mankey², J. Lee³, T. Lee³ and T. Lim³. *1. Department of Electrical and Computer Engineering, The University of Alabama, Tuscaloosa, AL, United States; 2. Department of Physics and Astronomy, The University of Alabama, Tuscaloosa, AL, United States; 3. Institute of Fundamental and Advanced Technology (IFAT), Hyundai Motor Company, Uiwang, The Republic of Korea*

Recently, Ke proposed alnico permanent magnet (PM) model and simulated it using micromagnetic simulation (MS) for magnetic properties [1]. The model is based on the branch (B) on the bottom (U-shaped), the top and bottom (O-shaped), and the middle (H-shaped) on Z-axis. The U-shaped and O-shaped alnico structures showed low coercivity (H_{ci}). However, there is still a lack of comprehensive studies on B dimensions such as B thickness (T_B), width (W_B), and length (L_B) when α_1 -phase rods experience coherent rotation and curling [2-4]. Further, the B can be formed as a Y-shaped structure during the thermal magnetic process [3,4]. We have simulated the effects of T_B , W_B , and L_B on H_{ci} for five structures, including H-, U-, O-, YU-, and YH-structures, using LLG micromagnetic simulator v2.63b [5]. Fig. 1 shows the alnico structures used in the simulation. For all structures, α_1 -phase rod having a diameter ($D_{\alpha 1}$) of 10 nm was used, representing coherent rotation. The simulation setup used in [1] is adopted. Fig. 2 shows the H_{ci} as a function of T_B , L_B , and W_B for $D_{\alpha 1}$ of 10 nm. As the T_B increases, the H_{ci} first decreases and then remains constant for all the structures. For L_B , a positive linear trend of H_{ci} is found for H- and Y-shaped structures, while there is a negative linear trend for the other two structures. As the W_B increases, nearly constant H_{ci} appears for the H- and Y-shaped structures, but for the U- and O-shaped structures, the H_{ci} shows a positive quadratic trend. As a simulation result, the following dimensions are suggested to realize a high H_{ci} of Alnico PM: thin T_B , long L_B , and W_B with 40 % of $D_{\alpha 1}$ for the H- and Y-shaped structures and thin T_B , short L_B , and W_B with 40-60 % of $D_{\alpha 1}$ for the U- and O-shaped structures. Furthermore, among the five studied structures, the B on the middle location of either H- or YH-shaped is desired to realize a high H_{ci} . We will further discuss the alnico PM rod experiencing curling. This work was supported in part by NSF-IUCRC for EV-STs under Grant No. 1650564.

[1] L. Ke, R. Skomsi, T. Hoffmann, *Applied Physics Letter*, 111, 022403 (2017). [2] H. Won, Y. K. Hong, M. Choi, *IEEE Magnetic Letters*, 12, 7501505 (2021). [3] S. Zhu, J. Zhao, W. Xia, *Journal of Alloys and Compounds*, 720, 401 (2017). [4] C. Zhang, Y. Li, X. Han, *Journal of Magnetism and Magnetic Materials*, 451, 200 (2018). [5] M. R. Scheinfein, LLG Micromagnetic Simulator™ [Online]. Available: <http://llgmicro.home.mindspring.com>